



HAL
open science

Robust synchronization of different coupled oscillators: Application to antenna arrays

Florin Doru Hutu, Sébastien Cauet, Patrick Coirault

► **To cite this version:**

Florin Doru Hutu, Sébastien Cauet, Patrick Coirault. Robust synchronization of different coupled oscillators: Application to antenna arrays. *Journal of The Franklin Institute*, 2009, 346 (5), pp.413-430. 10.1016/j.jfranklin.2009.01.001 . hal-01007680

HAL Id: hal-01007680

<https://hal.science/hal-01007680v1>

Submitted on 17 Jun 2014

HAL is a multi-disciplinary open access archive for the deposit and dissemination of scientific research documents, whether they are published or not. The documents may come from teaching and research institutions in France or abroad, or from public or private research centers.

L'archive ouverte pluridisciplinaire **HAL**, est destinée au dépôt et à la diffusion de documents scientifiques de niveau recherche, publiés ou non, émanant des établissements d'enseignement et de recherche français ou étrangers, des laboratoires publics ou privés.

Robust synchronization of different coupled oscillators: application to antenna arrays

Florin HUTU Sebastien CAUET Patrick COIRAULT

*University of Poitiers, Laboratoire d'Automatique et d'Informatique Industrielle, 40
Avenue du Recteur Pineau, 86022 Poitiers Cedex France*

Abstract

This paper treats the synchronization of a chain of non linear and uncertain model of non identical oscillators. Using the Lyapunov theory of stability, a dynamical controller guaranteeing the oscillators synchronization is determined. The problem of synchronization is transformed in a problem of asymptotic stabilization for a nonlinear system and then is formulated as a system of linear matrix inequalities where the parameter variations of the two oscillators and their differences are modeled by polytopic matrices. The theoretical result is successfully applied to an array of transistor-based oscillators used in "smart antenna" systems.

Key words: LMI , Robust control, Control applications, Antenna arrays

1 Introduction

The demand of mobile communication services is in a continuous growth, moreover, it is estimated that the rate will be maintained in the next years. This continuous development has stimulated the research of new hardware and software solutions in order to increase the volume of exchanged data and a better management of the emitted or received electromagnetic field.

Smart antennas are a part of communication systems that can help improve their global performances. These devices can increase the spectral efficiency and reduce the multi path fading, bit error rate (BER), the co-channel interferences (CCI) and the system complexity (Godara, 1997). This is possible by electronically adjusting their radiation patterns in order to present important gain for the desired signals and small gain for interference signals.

Email address: florin.hutu@etu.univ-poitiers.fr (Florin HUTU).

One of the challenges to control such devices is to generate signals with the same frequency and different phases and amplitudes. This paper proposes variation of a technique inspired from radar applications: the generation of synchronized and phase shifted signals using arrays of coupled non linear oscillators.

The work that has been done in the field of dynamics of coupled nonlinear oscillators using a harmonic approach (Guan et al., 2004; Hwang and Myung, 1998; Liao and York, 1993, 1994; Tombak and Mortazawi, 2003; York and Itoh, 1998; York and Popovic, 1997) has shown that they offer simple methods of phase control among array elements and hence beam scanning capabilities but also implies problems of stabilization. This paper treats the synchronization of a system made by two oscillators with a unidirectional coupling and this problem of synchronization is transformed in a problem of stabilization for a nonlinear system. The strategy chosen is to find an output feedback dynamic controller using Lyapunov functions.

The problem of calculating dynamic output feedbacks on LTI (linear time invariant) systems in term of matrix inequalities is difficult to solve. In fact this solution can be found by solving a set of bilinear matrix inequalities (BMI). There are two known techniques: the iterative algorithms and the elimination of variable products by using the matrix separation lemma. It has been chosen the second method who, in certain cases, transforms the initial BMI into a set of LMI-s who can be numerically solved (Arzelier et al., 2002; Arzellier et al., 2003; Mehdi et al., 2003; Iwasaki et al., 1998; Peaucele and Azellier, 2001; Boyd et al., 1994).

This technique involves the use of Lyapunov functions that depend on the polytopic structure of the uncertainty in order to reduce the conservatism of the method. This work refers to the results of (Peaucelle, 2000). The reader is invited to see (Geromel et al., 1998; Feron et al., 1996; Chilali et al., 1999; Peaucelle et al., 2000) where tractable results relevant to parameter-dependent Lyapunov functions are proposed.

It was demonstrated in (Geromel et al., 1998) and (de Oliveira et al., 1999) that the polytopic structure reduces conservatism. This improvement has been numerically verified in (Bachelier et al., 1999). In the discrete case, it exists a less pessimistic condition which consists on increasing the number of variables in LMI (Leite and Peres, 2003; Ramos and Peres, 2001). The originality of this paper comes from using both kind of uncertainties (polytopic and nonlinearity bound) and solving the problem of synchronization using the interior point techniques.

The variation of the parameters is taken into account by considering the state matrix as a polytopic one. Once the stability of the vertices, defined for the polytope is demonstrated, the stability and hence the synchronization of the two oscillators is assured for all systems inside the polytope.

The nonlinear character of the oscillators allows the synchronization (if their free running frequencies are in a certain domain (Liao and York, 1994)) but also makes them dependent of initial conditions. The main objective is to eliminate the non-

linear effect and to maintain the synchronization when the physical parameters of the oscillators and external conditions are modified. The originality of the method comes from the inclusion of the non-linear term and the undesired variations in a perturbation. This problem is transformed in a \mathcal{H}_∞ optimization.

In section 2 is presented an overview of the antenna array theory. In section 3 a theory of dynamical controller design for this particular class of nonlinear systems is developed. Section 4 presents the numerical results in the case of an array of coupled nonlinear oscillators.

2 Antenna array theory overview

In this section, a brief overview on the antenna array theory is given. It will be shown how, by controlling the phases and amplitudes of the carrier signals associated to each elementary antenna, the directional gain can be controlled.

Generally, a unspecified volume in the space who is able to emit electromagnetic radiation is formed by an infinity of elementary electrical dipoles. If it is considered that the radiation of a elementary dipole does not influence the others in the volume, the total emitted electromagnetic radiation is the weighted sum of the electromagnetic fields radiated by all dipoles.

A smart antenna is composed by an array of individual radiative elements (elementary antennas), which are disposed in a particular configuration (linear, circular or matrix). By grouping these elementary antennas in such arrays and by changing the characteristics of the signals associated to each element, the array can present different gains according to the direction. These gains are represented in so called radiation patterns and, because of the property of the reciprocity of the antennas (Harrington-Villeneuve principle), the radiation patterns are the same at the emission as at reception.

Let us consider an uniform linear array of N identical patch antennas placed at the same distance d between them as in Fig. 1.

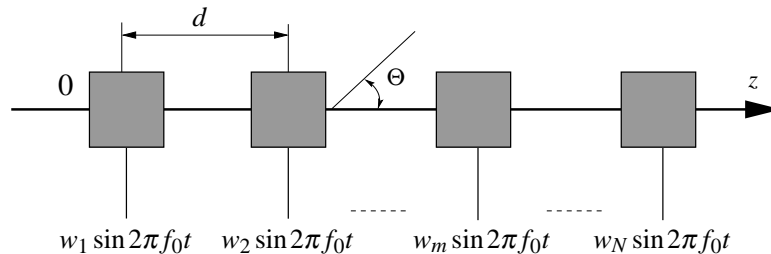


Fig. 1. An uniform antenna array

For the theoretical study of this configuration, it is supposed that in the elementary antennas, harmonic signals of the same frequency but different amplitudes and phases are injected.

The electromagnetic field of the antenna arrays is composed by a term who depends on the amplitudes and phases of the injected signals:

$$\mathbb{E}_{total} = \mathbb{E}_{ref} * f(\Theta) \quad (1)$$

Where \mathbb{E}_{ref} is the electromagnetic field of an elementary antenna and the array factor can be written as follows:

$$f(\Theta) = \sum_{m=1}^N \mathbf{w}_m e^{-j(m-1)k_0 d \cos \Theta} \quad (2)$$

This equation shows that the only way to modify the spatial distribution of the electromagnetic field is to modify the value of the array factor $f(\Theta)$. This became possible by changing the values of the \mathbf{w}_m complex coefficients.

2.1 Emission case

In the simplest case, in order to steer the main lobe of the radiation pattern in a unspecified direction Θ_{nec} , the carrier signals associated to each elementary antenna must verify two conditions:

- the amplitudes must have the same value. Usually it is considered $A_i = \frac{1}{N}$.
- the phase difference between two consecutive signals must be the same: $\Delta\varphi = \varphi_{i+1} - \varphi_i = c\tau; \forall i \in [1 \dots N]$

In this particular case, the mathematical expression of the radiation pattern is:

$$f(\theta) = \frac{1}{N} \frac{\sin \frac{N\gamma}{2}}{\sin \frac{\gamma}{2}} \quad (3)$$

where $\gamma = \varphi - k_0 d \cos(\theta)$; N the number of antennas, d the distance between them. It can be seen that a quantity of the radiated energy is lost in the side lobes which implies a certain weakening of the antenna array gain.

For the theoretical study, the Chebyshev method is considered. The same example of N equally spaced antennas, placed at the same distance $d = \frac{\lambda}{2}$ between them is considered. The reference antenna is located into the middle of the array and a

constant phase gradient is assumed: $\varphi_m - \varphi_{m-1} = \delta; \forall m \in \{-N/2, N/2\}$.

$$\begin{cases} f(\Theta) = 2 \sum_{m=0}^{n-1} A_m T_{2m+1}(w) & n = \frac{N}{2} \\ f(\Theta) = \sum_{m=0}^n A_m T_{2m}(w) & n = \frac{N-1}{2} \end{cases} \quad (4)$$

where $T_n(x)$ represents the Chebyshev polynomial of order n and variable x .

The variable w is defined as follows:

$$w = \cos\left(\frac{\delta - k_0 d \cos \Theta}{2}\right). \quad (5)$$

Fig. 2 presents the array factor and the radiation pattern when $R = \frac{L_{ML}}{L_{SL}} = 2$. The maximum in $\Theta = 60^\circ$ direction is tackled when a phase gradient δ of 90° is assured.

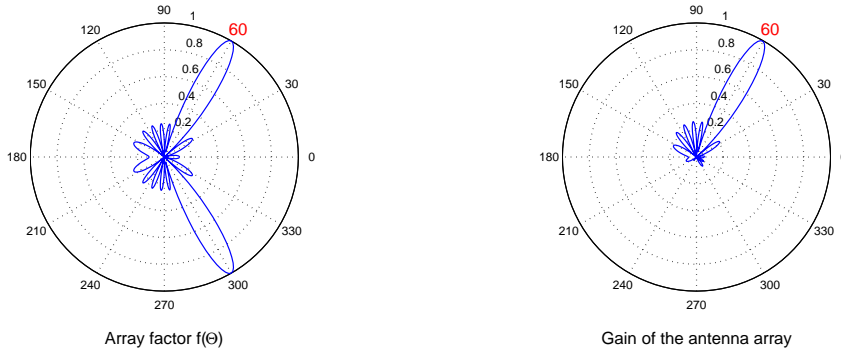


Fig. 2. The array factor and the gain of antenna array in the case of $N = 8$ patch antennas and Dolph-Chebyshev optimization

2.2 Estimation of direction of arrival

In modern communication systems, it is often used the principle of channel re-use. That means that neighbor clusters use the same communication channel and so, the signal to noise ratio become weak. In order to solve this problem, the antenna array can be able to present different directional gains; moreover, the system must be able to dynamically modify this gain in order to follow the useful link. The following example shows how such antennas are able to accomplish this task.

Let us consider the same array of $N = 8$ identical antennas placed at the same distance $d = \frac{\lambda_0}{2}$ between them ($f_0 = 2GHz$). It is supposed also that there is one

privileged signal having the angle of the position vector varying in interval $\Theta_p \in [0^\circ \dots 75^\circ]$. There are supposed two others fixed interference signals i_1 and i_2 having the angle of the position vector at $\Theta_{i1} = 90^\circ$ and $\Theta_{i2} = 120^\circ$ respectively, as in fig. 3.

The antenna array is supposed to present a certain gain in the direction of the privileged signal and to cancel the interference signals by presenting a null gain in their direction. The algorithm is initialized with a random set of weighting \mathbf{w} and at each variation of the privileged signal direction.

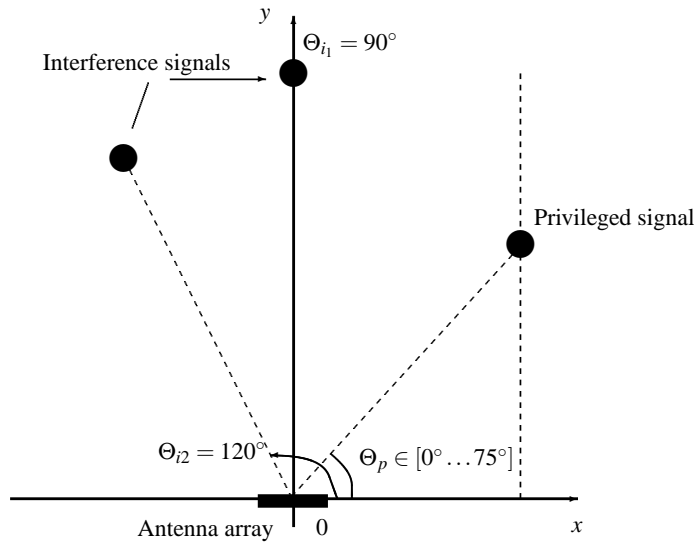


Fig. 3. Typical problem of DOA technique

Fig.4 presents the amplitudes and phases variations needed by the eight carrier signals in order to follow the useful signal and to eliminate the two other interferences. It can be seen that the variations are dispersed in the entire trigonometric circle.

Using these two examples, it can be seen that the both variations of the amplitudes and the phases of the carrier signals are in a large interval. This paper proposes a new technique to generate such signals having the same frequency and different

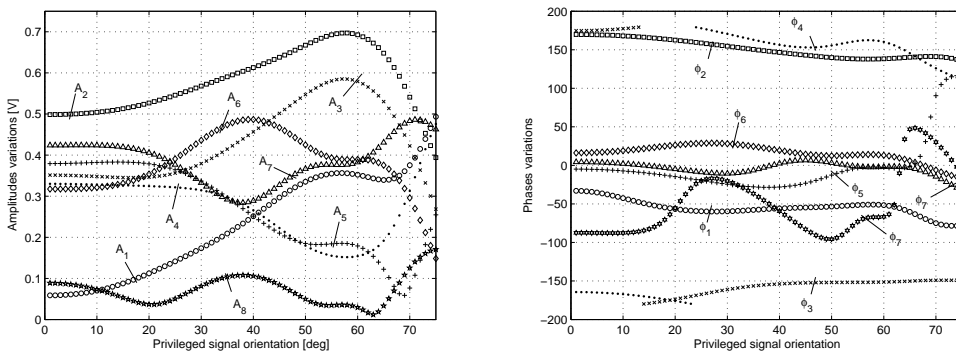


Fig. 4. The amplitudes and phases variations

phases and amplitudes.

3 Problem formulation

3.1 Problem statement

One can conclude that both variation of the amplitudes and phases are in a large interval. If the amplitude variation can be easily solved by using variable gain amplifiers, the problem of the phase variation is more constraining.

There are several techniques who permits solving this problem. These techniques can be divided in two main approaches: one which use the signal generated by one oscillator and the second who use signals generated by array of coupled oscillators.

Signals with the same frequency but different phases and amplitudes can be built by delaying the signal generated with one master oscillator using high-frequency power dividers and variable delay lines or Butler couplers. This approach is very useful when discrete systems are conceived. Another approach is to use polyphasic oscillators and a multiplexing system (Guan et al., 2004). The disadvantage of these techniques is that it cannot be obtained continuous phase variations.

The second approach is based on the synchronization of arrays of oscillators having their free running frequencies with a weak dispersion. In (Liao and York, 1994; York and Itoh, 1998) it was demonstrated that arrays of coupled nonlinear oscillators can synchronize, moreover, according to the coupling strength and to free-running frequencies, phase variations can be assured. Recent works (Heath, 2005) presents how the phase variation can be assured by changing only the free-running frequencies of all coupled oscillators in the array.

In this paper, the problem of generating the carrier signals with the same frequency and different phases is treated. In order to generate these carrier signals, the following general schematic Fig. 5 is proposed:

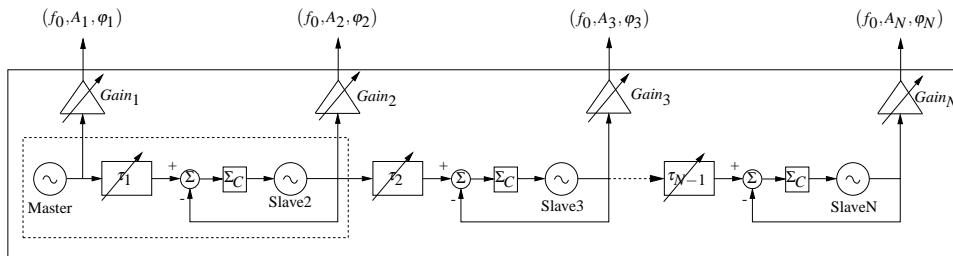


Fig. 5. Unidirectional coupling of a chain of oscillators

This schematic is a variation of the York's approach presented in (York, 1993).

Because of the unidirectional coupling, each slave oscillator is driven only by its left neighbor so, the study of this configuration is reduced to the study of a pair of two non-linear systems like in Fig. 6.

The purpose is to design the parameters of the Σ_C system in order to make the $y_e(t)$ output to tend toward zero. When this objective is accomplished, the delayed output of the master oscillator and the output of the slave oscillator becomes identical, so the two oscillators are synchronized.

Generally, because of the technological realization, the oscillators don't have the same free running frequencies. This is the reason why the feedback loop was introduced: to guarantee the robust synchronization between the two oscillators. The delay element and the variable gain amplifier will assure different phases and amplitudes for the output signals.

The difference between the oscillators will be modeled as a variation of the slave oscillator's parameters around those of the master oscillator parameters, which is considered as the reference. The variations due to the temperature or at the ageing of the components are modeled by a polytopic uncertainty of the master oscillator parameters around the nominal values.

In order to model the two oscillators, a class of nonlinear, uncertain systems having the following state-space representation will be considered:

$$\begin{cases} \dot{x} = A(\theta_1)x + g(x, t, \theta_1) + Bu \\ y = Cx \end{cases} \quad (6)$$

The $x \in \mathbb{R}^{n_x}$ vector represents the state vector, $u \in \mathbb{R}^{n_u}$ the input vector and $y \in \mathbb{R}^{n_y}$, the output vector. The vectorial function $g(x, t, \theta_1) : \mathbb{R}^{n_x} \times \mathbb{R} \times \mathbb{R}^M \mapsto \mathbb{R}^{n_x \times 1}$ is supposed to be a continuous function. The vector θ_1 has the size M and it contains all the uncertain parameters of the state matrix.

Assume that $A(\theta_1)$ is a matrix who belongs to a set \mathcal{A} defined as in (7). This set is a polytope of matrices and it represents a convex combination of the extreme matrices A_i , $i = 1 \dots 2^M$, the vertices of \mathcal{A} .

$$\mathcal{A} = \left\{ A(\theta_1) \mid A(\theta_1) = \sum_{i=1}^{2^M} \xi_i A_i; \xi_i \in \Delta_1 \right\} \quad (7)$$

with:

$$\Delta_1 = \left\{ \begin{bmatrix} \xi_1 \\ \vdots \\ \xi_{2^M} \end{bmatrix} \in \mathbb{R}^{2^M} \mid \xi_i \geq 0; \forall i \in 1 \dots 2^M; \sum_{i=1}^{2^M} \xi_i = 1 \right\} \quad (8)$$

The structure represented in Fig. 6 is made by two different systems who belongs to the class previously described. The master system is considered independent ($u = 0$) and the dynamical controller Σ_C drives the slave system using the error signal as reference. The error signal is constituted by the difference between a delayed version of the master's output and the slave's output.

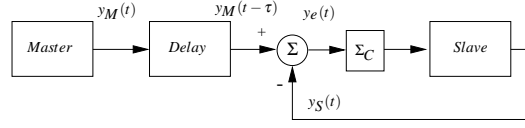


Fig. 6. Master-slave synchronization

The state-space representation of the master system can be written as follows:

$$\Sigma_M : \begin{cases} \dot{x}_M = A_M(\theta_1)x_M + g_M(x_M, t, \theta_1) \\ y_M = Cx_M \end{cases} \quad (9)$$

For the slave system, the state-space representation can be written as:

$$\Sigma_S : \begin{cases} \dot{x}_S = A_S(\theta_1)x_S + g_S(x_S, t, \theta_1) + B_2u \\ y_S = Cx_S \end{cases} \quad (10)$$

It is considered that between the state matrices A_M and A_S there is a small variation described by $B_1(\theta_2)$ matrix:

$$A_M(\theta_1) = A_S(\theta_1) + B_1(\theta_2) \quad (11)$$

The vector θ_2 has the size $P \leq M$ and it contains all the parameters in θ_1 that varies from the master system to the slave one.

The matrix $B_1(\theta_2)$ also belongs to a set \mathcal{B}_1 defined as follows:

$$\mathcal{B}_1 = \left\{ B_1(\theta_2) \mid B_1(\theta_2) = \sum_{i=1}^{2^P} \zeta_i B_{1i}; \zeta_i \in \Delta_2 \right\} \quad (12)$$

with:

$$\Delta_2 = \left\{ \begin{bmatrix} \zeta_1 \\ \vdots \\ \zeta_{2^P} \end{bmatrix} \in \mathbb{R}^{2^P} \mid \zeta_i \geq 0; \forall i \in 1 \dots P; \sum_{i=1}^{2^P} \zeta_i = 1 \right\} \quad (13)$$

Let us note the non linearities difference as follows:

$$g_M(x_M, t, \theta_1) - g_S(x_S, t, \theta_1) = e_g(x_M, x_S, t, \theta_1) \quad (14)$$

and let us consider that the matrix $e_g(x_M, x_S, t, \theta_1)$ can be bounded, $N_B(\theta_1)$ being its upper bound:

$$N_B(\theta_1)e \leq e_g(x_M, x_S, t, \theta_1) \quad (15)$$

$N_B(\theta_1)$ is a time invariant matrix who belongs to a polytope $\mathcal{N}_{\mathcal{B}}$:

$$\mathcal{N}_{\mathcal{B}} = \left\{ N_B(\theta_1) \mid N_B(\theta_1) = \sum_{i=1}^{2^M} \xi_i N_{Bi}; \xi_i \in \Delta \right\} \quad (16)$$

where Δ_1 defined as in (8).

Remark 1 $A(\theta_1)$ and $N_B(\theta_1)$ are two polytopic matrices that depends on the same parameters θ_1 . The sum $A_N(\theta_1) = A(\theta_1) + N_B(\theta_1)$ is a polytopic matrix, $A_N(\theta_1) \in \mathcal{A}_{\mathcal{N}}$, where:

$$\mathcal{A}_{\mathcal{N}} = \left\{ A_N(\theta_1) \mid A_N(\theta_1) = \sum_{i=1}^{2^M} \xi_i A_{Ni}; \xi \in \Delta \right\} \quad (17)$$

where $A_{Ni} = A_i + N_{Bi}$

If an error state is defined as

$$e(t) = x_M(t - \tau) - x_S(t), \quad (18)$$

a state-space representation can be written:

$$\Sigma_e : \begin{cases} \dot{e} = A_N(\theta_1)e - B_1(\theta_2)x_S - B_2u \\ y_e = Ce \end{cases} \quad (19)$$

3.2 Controller synthesis

Assume that the dynamical output controller has the following state-space representation and its dimension is n_c :

$$\Sigma_C : \begin{cases} \dot{x}_c = A_c x_c + B_c y_e \\ u = C_c x_c + D_c y_e \end{cases} \quad (20)$$

The purpose of this controller is to force the slave system to follow the delayed output of the master system. This condition is accomplished when the error signal defined in (18) tends toward zero. The term $B_1(\theta_2)x_s$, representing the difference between the two systems, acts like a perturbation on the error state e . In order to reject this perturbation, the T_∞ transfer between the Z_∞ output defined in (21) and the x_s state, will be minimized (22).

$$Z_\infty = C_\infty e \quad (21)$$

where $C_\infty = \begin{bmatrix} 1 & 0 \\ 0 & 1 \end{bmatrix}$.

The transfer T_∞ is defined as follows:

$$T_\infty = \frac{\|Z_\infty\|_\infty}{\|x_s\|_\infty} < \gamma^2 \quad (22)$$

This is a classical \mathcal{H}_∞ problem who consists in finding the controller K and the real scalar γ as small as possible:

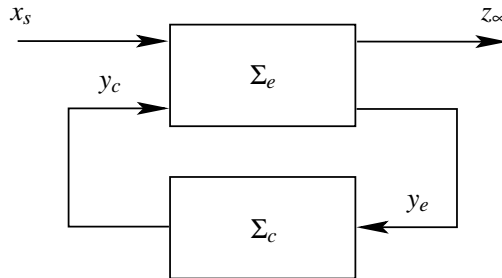


Fig. 7. \mathcal{H}_∞ principle

The closed loop system can be described by the following state-space representa-

tion:

$$\begin{cases} \dot{x}_{cl} = A_{cl}(\theta_1)x_{cl} + \tilde{B}_1(\theta_2)x_s \\ z_\infty = C_{cl}x_{cl} \end{cases} \quad (23)$$

where: $A_{cl} = \tilde{A}_N(\theta_1) + \tilde{B}_2K\tilde{C}$; $C_{cl} = [C_\infty \quad \mathbb{O}]$ and:

$$z = \begin{bmatrix} e \\ x_c \end{bmatrix} \quad \tilde{A}_N(\theta_1) = \begin{bmatrix} A_N(\theta_1) & \mathbb{O} \\ \mathbb{O} & \mathbb{O} \end{bmatrix} \quad \tilde{B}_2 = \begin{bmatrix} -B_2 & \mathbb{O} \\ \mathbb{O} & \mathbb{I} \end{bmatrix} \quad (24)$$

$$K = \left[\begin{array}{c|c} D_c & C_c \\ \hline B_c & A_c \end{array} \right] \quad \tilde{C} = \begin{bmatrix} C & \mathbb{O} \\ \mathbb{O} & \mathbb{I} \end{bmatrix} \quad \tilde{B}_1(\theta_2) = \begin{bmatrix} B_1(\theta_2) \\ \mathbb{O} \end{bmatrix}$$

Using the real bound lemma (see(Chilali et al. (1999); Boyd et al. (1994))), the condition (22) applied to the closed loop system (23) can be written as follows:

$$\begin{bmatrix} A_{cl}(\theta_1)^T P(\theta_1) + P(\theta_1)A_{cl} & P(\theta_1)\tilde{B}_1(\theta_2) & C_{cl}^T \\ \tilde{B}_1(\theta_2)^T P(\theta_1) & -\gamma\mathbb{I} & \mathbb{O} \\ C_{cl} & \mathbb{O} & -\gamma\mathbb{I} \end{bmatrix} \leq \mathbb{O} \quad (25)$$

where $P(\theta_1)$ is a positive definite, symmetric and parameter-dependent matrix defined by:

$$P(\theta_1) = \sum_{i=1}^{2^M} \xi_i P_i \quad (26)$$

To study the stability of this system, the stability of the extreme matrices A_{N_i} , the vertices of \mathcal{A}_N should be studied.

Assumption 1 *It is supposed that it exists a stabilizing state feedback controller K_0 that is the solution of the following LMI:*

$$\begin{bmatrix} A_{cl}(\theta_1)X + XA_{cl}^T + \tilde{B}_2L_0 + (\tilde{B}_2L_0)^T & \tilde{B}_1(\theta_2) & XC_{cl}^T \\ \tilde{B}_1(\theta_2) & -\gamma_0\mathbb{I} & \mathbb{O} \\ C_{cl}X & \mathbb{O} & -\gamma_0\mathbb{I} \end{bmatrix} \leq \mathbb{O} \quad (27)$$

where X is a symmetric, positive definite matrix, having the same dimensions as $P(\theta_1)$. The state feedback controller K_0 is solution of $L_0 = K_0X$.

The $P(\theta_1)$ and K unknown variable matrices and the unknown positive constant γ that makes the (25) inequality feasible, can be calculated only in the vertices of \mathcal{A} and \mathcal{B}_1 , sight that each value $\tilde{A}(\theta_1)$ and $\tilde{B}_1(\theta_2)$ can be written as a convex combination of those vertices.

The following theorem solves the problem of variable matrices product in (25) by introducing extra unknown variable matrices. The equivalent expression (28) of (25) can be numerically solved using Matlab's[©] "LMI Toolbox".

Theorem 1 *If there exists a set of matrices $P_i > 0$, a matrix K_0 that is solution of (27), a unknown variable square and nonsingular matrix $G \in \mathbb{R}^{n_u+n_c}$, a unknown variable matrix $H \in \mathbb{R}^{(n_u+n_c) \times (n_u+n_c)}$ and four unknown variables matrices $F_1, F_4 \in \mathbb{R}^{(n_x+n_c) \times (n_x+n_c)}$, $F_2 \in \mathbb{R}^{n_x \times (n_x+n_c)}$ and $F_3 \in \mathbb{R}^{(n_\infty+n_c) \times (n_x+n_c)}$ such that the inequality (28) is verified, then the dynamical controller $K = G^{-1}L$ makes the error system (19) asymptotically stable for all matrices $A_N(\theta_1)$ and $B_1(\theta_2)$ described as convex combination of the elements in \mathcal{A}_N and \mathcal{B}_1 respectively and with respect of (22) condition.*

$$\begin{aligned} \Phi_2 + {}^1\text{Sym} \left\{ \begin{array}{c} \left[\begin{array}{c} F_1 \\ F_2 \\ F_3 \\ F_4 \\ \mathbb{O} \end{array} \right] \left[\begin{array}{cccccc} \mathbb{O} & \mathbb{O} & \mathbb{O} & \mathbb{O} & \mathbb{O} & \tilde{B}_2 \end{array} \right] \\ \left[\begin{array}{c} \mathbb{O} \\ \mathbb{O} \\ \mathbb{O} \\ \mathbb{O} \\ \mathbb{I} \end{array} \right] L \left[\begin{array}{cccccc} \tilde{C} & \mathbb{O} & \mathbb{O} & \mathbb{O} & \mathbb{O} & \mathbb{O} \end{array} \right] \end{array} \right\} \\ + \text{Sym} \left\{ \begin{array}{c} \left[\begin{array}{c} \mathbb{O} \\ \mathbb{O} \\ \mathbb{O} \\ \mathbb{O} \\ \mathbb{I} \end{array} \right] G \left[\begin{array}{cccccc} -K_0 & \mathbb{O} & \mathbb{O} & \mathbb{O} & \mathbb{O} & -\mathbb{I} \end{array} \right] \end{array} \right\} < \mathbb{O}; \end{aligned} \quad (28)$$

¹ $\text{Sym}\{X\} = X^T + X; \forall X \in \mathbb{R}^n$

The matrix Φ_2 is defined as follows:

$$\Phi_2 = \begin{bmatrix} \mathbb{O} & \mathbb{O} & C_{cl}^T & P_i & \mathbb{O} \\ \mathbb{O} & -\gamma\mathbb{I} & \mathbb{O} & \mathbb{O} & \mathbb{O} \\ C_{cl} & \mathbb{O} & -\gamma\mathbb{I} & \mathbb{O} & \mathbb{O} \\ P_i & \mathbb{O} & \mathbb{O} & \mathbb{O} & \mathbb{O} \\ \mathbb{O} & \mathbb{O} & \mathbb{O} & \mathbb{O} & \mathbb{O} \end{bmatrix} + \text{Sym} \left\{ \begin{bmatrix} F_1 \\ F_2 \\ F_3 \\ F_4 \\ \mathbb{O} \end{bmatrix} \left[\tilde{A}_{0i} \tilde{B}_{1j} \mathbb{O} -\mathbb{I} \mathbb{O} \right] \right\} \quad (29)$$

$\forall i \in \{1 \dots 2^M\}$ and $\forall j \in \{1 \dots 2^P\}$

Where $\tilde{A}_{0i} = \tilde{A}_{Ni} + \tilde{B}K_0$. Let us introduce the following notation:

$$S = K\tilde{C} - K_0 \quad (30)$$

See Proof in the appendix.

4 Numerical results

In order to verify the theoretical result, a transistor-based simulation has been done using Agilent's ADS[®] software and models of MOSFET transistors in $0.35\mu\text{m}$ silicon technology. The oscillators are conceived using a double differential pair structure. In order to determine the value of the dynamical controller, the non linear oscillators were modeled using the van der Pol model. This model is composed by an ideal resonant circuit coupled with a nonlinear element having the following conductance: $g(v) = -\alpha + \beta v^2$; $\alpha, \beta \in \mathbb{R}_+^*$.

The parameters $\alpha = 0.379$ and $\beta = 0.281$ were identified using a simple least square algorithm and the current-voltage characteristic provided by the differential pair of transistors. The values for the components of the resonant circuit ($L_0 = 6,33\text{nH}$ and $C_0 = 1\text{pF}$) are chosen to assure $f_0 = 2\text{GHz}$ output frequency.

4.1 The van der Pol model of a transistor based-oscillator

In order to model the non-linear behavior of the oscillators, the van der Pol model was used. There are two possible ways to write its state-space representation. The usual manner is to consider as state-space variables, the output tension and its derivative. In this article, the considered variables are the output tension v_0 and

the inductance current i_L :

$$\begin{cases} \frac{di_L}{dt} = \frac{1}{L_0}v_o \\ \frac{dv_o}{dt} = -\frac{1}{C_0}i_L + \frac{\alpha}{C_0}v_o - \frac{\beta}{C_0}v_o^3 + \frac{1}{C_0}i_{inj} \end{cases} \quad (31)$$

This system can be rewritten in a state-space form who is equivalent to the representation given in (6):

$$\begin{cases} \dot{x} = A(\theta_1)x + g(x, t, \theta_1) + Bu \\ y = Cx \end{cases} \quad (32)$$

where:

$$\begin{aligned} x &= \begin{bmatrix} i_L \\ v_o \end{bmatrix} & A(\theta_1) &= \begin{bmatrix} 0 & \frac{1}{L_0} \\ -\frac{1}{C_0} & 0 \end{bmatrix} \\ u &= \frac{i_{inj}}{C_0} & g(x, t, \theta_1) &= \begin{bmatrix} 0 \\ -\frac{\alpha}{C_0}x_2 + \frac{\beta}{C_0}x_2^3 \end{bmatrix} \\ B &= \begin{bmatrix} 0 \\ 1 \end{bmatrix} & C &= [0 \ 1] \end{aligned} \quad (33)$$

with the uncertain parameters: $\theta_1 = [\alpha, L_0, C_0]$.

It is considered the structure in fig. 6 made by two such oscillators and with the dynamical controller calculated with (28). Between the parameters of the master and the slave oscillators, it is considered that there is the same difference δ :

$$\begin{cases} L_S = L_M(1 + \delta) \\ C_S = C_M(1 + \delta) \\ \alpha_S = \alpha_M(1 + \delta) \\ \beta_S = \beta_M(1 + \delta) \end{cases} \quad (34)$$

This difference is translated into the difference between the A_M and A_S matrices as

in (11). With the assumptions in (34), $B_1(\theta_2)$ can be written as follows:

$$B_1(\theta_2) = \begin{bmatrix} 0 & -\frac{\delta}{L_M(1+\delta)} \\ \frac{\delta}{C_M(1+\delta)} & 0 \end{bmatrix} \quad (35)$$

4.2 Nonlinear bound determination

In order to determine the bounds of the nonlinearities difference, the scalar function $f: \mathcal{D}_1 \mapsto \mathcal{D}_2$; $f(x) = -\alpha x + \beta x^3$ is considered. The bounds can be considered as the slopes of the tangents at the graphical representation of $f(x)$ in the points $x = x_m$ and $x = 0$ as in Fig. 9.

$$-\alpha(x_2 - x_1) \leq (f(x_2) - f(x_1)) \leq (-\alpha + 3\beta x_m^2)(x_2 - x_1) \quad (36)$$

$$\forall x_1, x_2 \in \mathcal{D}_1$$

Fig. 8. The choice of the bound of the nonlinear function

If it is considered the case of the two nonlinear oscillators and the domain $\mathcal{D}_1 = [-1.35V, 1.35V]$, the bound of the nonlinearities difference (14) can be written as follows:

$$\begin{bmatrix} 0 \\ -\frac{1}{C_0}(\alpha + 3\beta - 0.2^2) \end{bmatrix} \leq N(x_M, x_S, t, \theta) \leq \begin{bmatrix} 0 \\ \frac{\alpha}{C_0} \end{bmatrix} \quad (37)$$

Fig. 9. The choice of the bound of the nonlinear function

In the worst case, the superior limit is taken and the matrix $A_N(\theta)$ becomes:

$$A_N(\theta) = \begin{bmatrix} 0 & -\frac{1}{L_0} \\ \frac{1}{C_0} & \frac{\alpha}{C_0} \end{bmatrix} \quad (38)$$

It was considered that all the parameters of $A_N(\theta)$ have $\pm 5\%$ variation around the nominal value. This variation can be seen as the variation depending on the temperature of the oscillators that are built on the same integrated circuit substrate. This is mathematically translated by the variation of the state matrix $A_N(\theta_1)$ inside the polytope \mathcal{A}_N . Using the Matlab's "LMI Toolbox" in order to solve the system of inequalities (28) applied to the 8 vertices of the polytope \mathcal{A}_N , the following state-feedback controller was found:

$$K = \left[\begin{array}{c|c} 2.66588 \cdot 10^{11} & 22.3994 \\ \hline 7.51499 \cdot 10^9 & -1.1885 \end{array} \right] \quad (39)$$

This controller has the structure given in (24) and the first order is chosen in respect of implementation constraints. It assures the synchronization of oscillators having $\delta = \pm 5\%$ difference between parameters. This difference is represented by variation of the perturbation matrix $B_1(\theta_2)$ inside the polytope \mathcal{B}_1 .

The difference between L_M, C_M and L_S, C_S parameters, translates a possible difference between the free-running frequencies of the two oscillators:

$$f_{0S} \in \left[f_{0M} (1 - |\delta|)^2 \quad f_{0M} (1 + |\delta|)^2 \right] \quad (40)$$

In our case the guaranteed synchronization interval is:

$$f_{0S} \in [0.9f_{0M} \ 1.1f_{0M}] \quad (41)$$

The difference between α_M, β_M and α_S, β_S translates a possible difference between the transistor operating points of the two non linear oscillators.

Fig. 10 presents the eigenvalues of the closed loop system (25) when $A_N(\theta_1)$ takes random values in the polytope \mathcal{A}_N . and $B_1(\theta_2)$ in the polytope \mathcal{B}_1 It can be seen that all the eigenvalues are in the left half-plan.

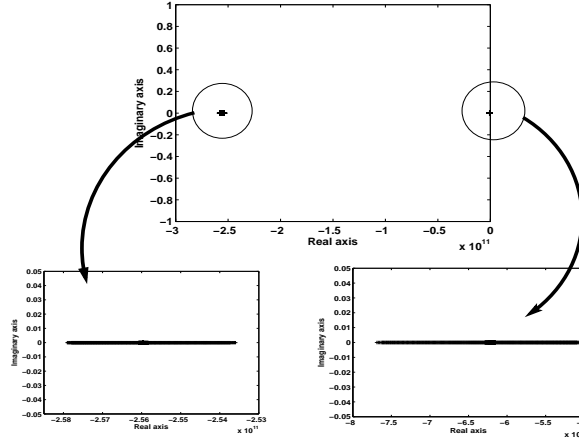


Fig. 10. The poles and the zeros of the closed loop system

The state controller K_0 that has been found and who permits the initialization of (28) LMI is:

$$K_0 = \begin{bmatrix} 2.33 \cdot 10^{11} & 6.25 \cdot 10^{10} & -5.26 & -0.54 \\ 6.76 \cdot 10^{11} & 1.17 \cdot 10^{11} & -8.09 & -0.24 \\ -1.22 \cdot 10^{10} & -1.89 \cdot 10^9 & 0.10 & -2.60 \end{bmatrix} \quad (42)$$

This controller was applied to a pair of two non-linear oscillators having coupled as in (6). Their free running frequencies are $f_{0M} = 2GHz$ and $f_{0S} = 2.2GHz$.

In fig. 12 there are presented the two output voltages for master and slave oscillators and is divided into three sequences:

- I. a first sequence in which, because the controller Σ_c is not activated, the two oscillators oscillates from their free-running frequencies: $f_M = 2.2GHz$ and $f_S = 1.8GHz$, the limits of the guaranteed region of synchronization (41).
- II. at $t = 55ns$, the controller Σ_c is activated. It can be seen that, after approximatively two periods, the two oscillators are synchronized at the master oscillator

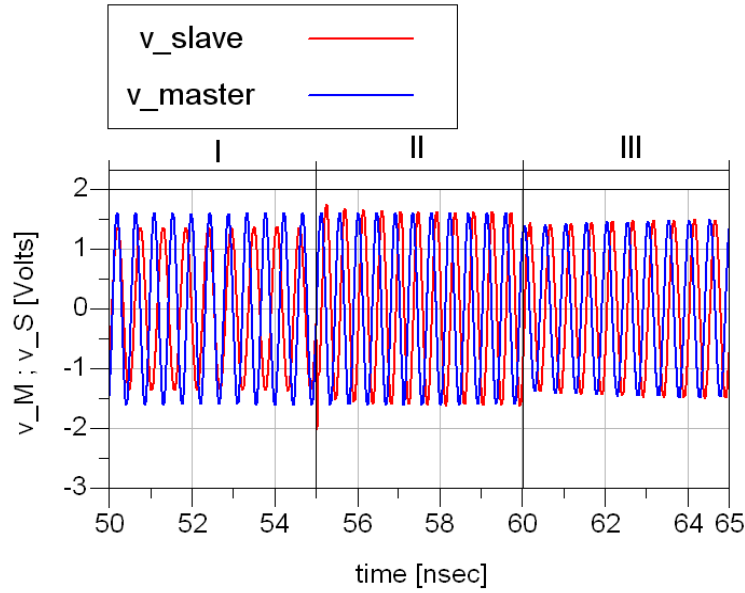


Fig. 11. Output tensions of the two oscillators

frequency: $f_M = f_S = 2.2GHz$. The obtained delay is closed to the imposed value ($\tau = T/4 = 1.25 \cdot 10^{-10}s$). This delay will correspond to a orientation of the main lobe in $\Theta = 120^\circ$.

- III. at $t = 60ns$, in order to verify the robustness of the dynamical controller, the free running frequency of the master oscillator was changed to $f_M = 2GHz$. It can be seen that the slave oscillator, after the transient regime, locks on the new reference: $f_M = f_S = 2GHz$.

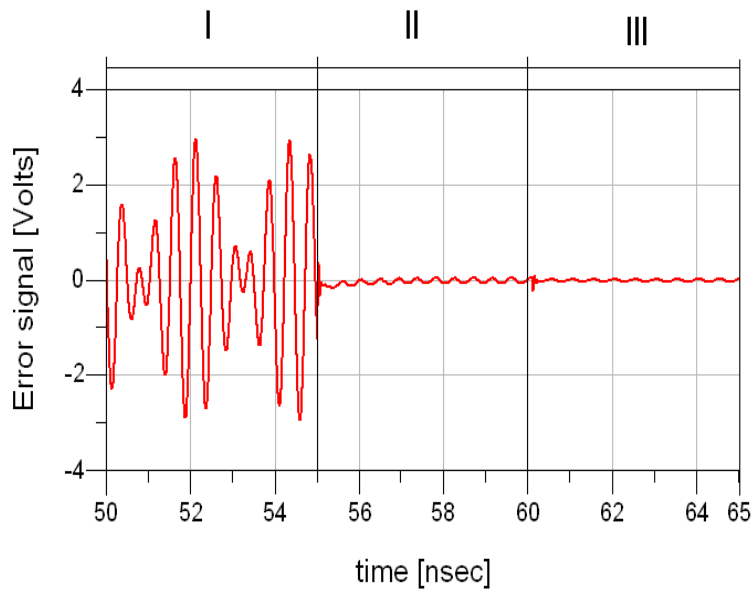


Fig. 12. The error between the two signals provided by the oscillators

In fig. 11 the error between the two output signals is presented. It can be seen

that the error tends toward zero after a short period of time after the controller's activation and the modification of master oscillator's frequency.

5 Conclusion

This paper presents a robust \mathcal{H}_∞ synthesis used to determine a dynamical controller who synchronize two non linear oscillators coupled by a delay line. The polytopic form of the system includes the variation of the physical parameters due to the temperature variation, to the uncertainties of the model and the oscillators differences. The proposed technique was successfully applied to a system of two coupled non linear oscillators. It has been extended successfully to a chain of eight unidirectionally coupled oscillators. Additional research will be made to constrain the dynamical controller to realize the desired delay in order to eliminate the delay element.

6 Appendix : Proof of theorem

PROOF. In order to prove this theorem, two particular forms of matrix separation lemma will be introduced. These lemmas permits to eliminate products of variables by increasing the order of the final system. Their demonstrations are given in (Iwasaki et al., 1998).

Lemma 2 *The two following affirmations are equivalent:*

1. *Let Φ , a and b , three matrices such that:*

$$\Phi + \text{Sym} \{ ab^T \} < 0$$

2. *Let Φ , a and b , three matrices such as the next LMI has a solution with G as variable:*

$$\left\{ \begin{array}{l} \left[\begin{array}{cc} \Phi & \mathbb{O} \\ \mathbb{O} & \mathbb{O} \end{array} \right] + \text{Sym} \left\{ \left[\begin{array}{c} a \\ \mathbb{O} \end{array} \right] \left[\begin{array}{cc} \mathbb{O} & \mathbb{I} \end{array} \right] \right\} + \text{Sym} \left\{ \left[\begin{array}{c} \mathbb{O} \\ \mathbb{I} \end{array} \right] G \left[\begin{array}{cc} b^T & -\mathbb{I} \end{array} \right] \right\} < 0 \\ \Phi < 0 \end{array} \right.$$

Lemma 3 *The two following affirmations are equivalent:*

1. Let Φ , a and b , three matrices such that the next LMI has a solution with f_1 and f_2 as variables:

$$\begin{bmatrix} \Phi & a \\ a^T & \mathbb{O} \end{bmatrix} + \text{Sym} \left\{ \begin{bmatrix} f_1 \\ f_2 \end{bmatrix} \begin{bmatrix} b^T & -\mathbb{I} \end{bmatrix} \right\} < 0$$

2. Let Φ , a and b , three matrices such that:

$$\Phi + \text{Sym} \{ab^T\} < 0$$

It is supposed that the inequality (28) is verified. Using the inverse form of **Lemma 2** for the triplet (ϕ_2, a_2, b_2) with:

$$a_2 = \begin{bmatrix} F_1 \tilde{B} \\ F_2 \tilde{B} \\ F_3 \tilde{B} \\ F_4 \tilde{B} \end{bmatrix} \quad \text{and} \quad b_2^T = [S \ \mathbb{O} \ \mathbb{O} \ \mathbb{O}] \quad (43)$$

the following equivalent inequality is obtained:

$$\begin{bmatrix} \mathbb{O} & \mathbb{O} & C_{cl}^T & P_i \\ \mathbb{O} & -\gamma \mathbb{I} & \mathbb{O} & \mathbb{O} \\ C_{cl} & \mathbb{O} & -\gamma \mathbb{I} & \mathbb{O} \\ P_i & \mathbb{O} & \mathbb{O} & \mathbb{O} \end{bmatrix} + \text{Sym} \left\{ \begin{bmatrix} F_1 \\ F_2 \\ F_3 \\ F_4 \end{bmatrix} \begin{bmatrix} \tilde{A}_{Ni} + \tilde{B}_2 K \tilde{C} & \tilde{B}_{1j} & \mathbb{O} & -\mathbb{I} \end{bmatrix} \right\} < \mathbb{O} \quad (44)$$

$\forall i \in \{1 \dots 2^M\}$ and $\forall j \in \{1 \dots 2^P\}$

Remark 2 The expression $\Phi_2 < \mathbb{O}$ is a equivalent form of the (27) inequality. This inequality is verified because it was supposed that it exists a stabilizing state feedback controller K_0 (see **Assumption 1**).

If we apply to the inequality in (44) the direct form of **Lemma 3** using (Φ_1, a_1, b_1^T) as variables, the equivalent form of (25) is obtained. The values for Φ_1 , a_1 and b_1^T are:

$$\Phi_1 = \begin{bmatrix} \mathbb{O} & \mathbb{O} & C_{cl}^T \\ \mathbb{O} & -\gamma \mathbb{I} & \mathbb{O} \\ C_{cl} & \mathbb{O} & -\gamma \mathbb{I} \end{bmatrix} \quad a_1 = \begin{bmatrix} P_i \\ \mathbb{O} \\ \mathbb{O} \end{bmatrix} \quad b_1^T = [\tilde{A}_{Ni} + \tilde{B}_2 K \tilde{C} \quad \tilde{B}_{1j} \quad \mathbb{O}] \quad (45)$$

The inequality in (25) proves the asymptotic stability of the system (27) in the vertex points of the polytopes \mathcal{A}_N and \mathcal{B}_1 . Or, each matrix $A_N(\theta_1)$ and $B_1(\theta_2)$ in the polytopes can be written as a convex combination of the limit points so the system (25) is asymptotically stable for all values inside those polytopes.

Using (27) a dynamical controller defined by (28) (and who can be seen as a filter having the transfer function like in (46)) can be calculated.

$$H(s) = C_C (s\mathbb{I} - A_C)^{-1} B_C + D_C \quad (46)$$

This dynamical controller guaranties the robust synchronization of the system presented in Fig.(6).

References

- L. C. Godara (Ed.), Applications of Antenna Arrays to Mobile Communications, Part I: Performance Improvement, Feasibility and System Consideration, Vol. 85, Proceedings of the IEEE, 1997.
- X. Guan, H. Hashemi, A. Hajimiri, A fully integrated 24 GHz eight-element phased-array receiver in silicon, IEEE Journal of Solid-State Circuits 39 (12) (2004) 2311–2320.
- J.-H. Hwang, N.-H. Myung, A new beam-scanning technique by controlling the coupling angle in a coupled oscillator array, IEEE Microwave and Guided Wave Letters 8 (5) (1998) 191–193.
- P. Liao, R. A. York, A new phase-shifterless beam-scanning technique using arrays of coupled oscillators, IEEE Transactions on Microwave Theory and Techniques 41 (10) (1993) 1810–1815.
- P. Liao, R. A. York, A six-element beam scanning array, IEEE Microwave and Guided Wave Letters 4 (1) (1994) 20–22.
- A. Tombak, A. Mortazawi, A novel low-cost beam-steering technique based on the extended resonance power dividing method, IEEE Transactions on Microwave Theory and Techniques (2003) 1–7.
- R. A. York, T. Itoh, Injection and phase-locking techniques for beam control, IEEE Transactions on Microwave Theory and Techniques 46 (11) (1998) 1920–1929.
- R. A. York, Z. B. Popovic, Active and quasi-optical arrays for solid-state power combining, John Wiley & Sons, Inc, 1997.
- D. Arzelier, D. Peaucelle, R. Ariza, Une methode iterative pour la synthese mixte $\mathcal{H}_2/\mathcal{H}_\infty$ par retour de sortie statique, CIFA 2002.
- D. Arzelier, D. Peaucelle, S. Salhi, Robust static output feedback stabilization for polytopic uncertain systems: improving the guaranteed performance bound, in: ROCOND Milan-Italy, 2003.

- D. Mehdi, E. Boukas, O. Bachelier, Static output feedback design for uncertain linear discrete time system, IMA Journal of Mathematical Control and Information.
- T. Iwasaki, R. E. Skelton, K. Grigoriadis., A unified algebraic approach to linear control design, Taylor and Francis, 1998.
- D. Peaucele, D. Azellier, An efficient numerical solution for \mathcal{H}_2 static output feedback synthesis, European Control Conference.
- S. Boyd, L. E. Ghaoui, E. Feron, V. Balakrishnan, Linear Matrix Inequalities in System and Control Theory, Vol. 15, Studies in Applied Mathematics, USA, 1994.
- D. Peaucelle, Formulation generique de problemes en analyse et commande robuste par des fonctions de lyapunov dependant de parametres, Phd thesis, University Paul Sabatier, Toulouse-France (July 2000).
- J. C. Geromel, M. de Oliveira, L. Hsu, \mathcal{LMI} characterization of structural and robust stability, Linear Algebra and its Applications 285 (1998) 69–80.
- E. Feron, P. Apkarian, P. Gahinet, Analysis and synthesis of robust control systems via parameter dependant lyapuonv functions, IEEE Trans. Aut. Control 41 (1996) 436–442.
- M. Chilali, P. Gahinet, P. Apkarian, Robust pole placement in \mathcal{LMI} regions, IEEE Trans. Aut. Control 44 (12) (1999) 2257–2269.
- D. Peaucelle, D. Arzelier, O. Bachelier, J. Bernussou, A new robust \mathcal{D} -stability condition for real convex polytopic uncertainty, Systems and Control Letters 40 (1) (2000) 21–30.
- M. C. de Oliveira, J. Bernussou, J. C. Geromel, A new discrete-time robust stability condition, Systems and Control Letters 37 (4).
- O. Bachelier, J. Bernussou, M. C. Oliveira, J. C. Geromel, Parameter dependant lyapunov design : numerical evaluation, in: Conference on Decision and Control, Phoenix, USA, 1999, p. Invited Session.
- V. S. J. Leite, P. L. D. Peres, An improved \mathcal{LMI} condition for \mathcal{D} -stability of uncertain polytopic systems, IEEE Trans. Aut. Control 48 (3) (2003) 500–504.
- D. C. W. Ramos, P. L. . D. Peres, A less conservative \mathcal{LMI} condition for the robust stability of discrete-time systems, Systems & Control Letters 43 (2001) 371–378.
- T. Heath, Simultaneous beam steering and null formation with coupled, nonlinear oscillator arrays, IEEE Transactions on Antennas and Propagation 53 (6) (2005) 2031–2035.
- R. A. York, Nonlinear analysis of phase relationships in quasi-optical oscillator arrays, IEEE Transactions on Microwave Theory and Techniques 41 (10) (1993) 1799–1809.

7 Reviewers comments

Reviewer 3: Fig.6 clearly shows that the error state equation (18) rather than the original (13) is used in the design of an H_∞ controller. The idea behind this is the nonlinearity within the system can be removed for the control system design. The authors claims the reason that this can be done is $\dot{V}(e)_{\sigma_e} \leq \dot{V}(e)_{\Sigma_e}$ due to (14). However this is not trivial and a proof is necessary.

Moreover, eqn 14 is very confusing. First, it needs to make clear what the inequality means in (14) because the involved quantities are vectors. Second, this inequality indicates the difference of the nonlinear parts between master and slave systems tends to zero when the two systems reach synchronization. Is it a realistic assumption?